



Lewis Acidity of Organofluorophosphonium Salts: Hydrodefluorination by a Saturated Acceptor

Christopher B. Caputo *et al.*

Science **341**, 1374 (2013);

DOI: 10.1126/science.1241764

This copy is for your personal, non-commercial use only.

If you wish to distribute this article to others, you can order high-quality copies for your colleagues, clients, or customers by [clicking here](#).

Permission to republish or repurpose articles or portions of articles can be obtained by following the guidelines [here](#).

The following resources related to this article are available online at www.sciencemag.org (this information is current as of December 3, 2013):

Updated information and services, including high-resolution figures, can be found in the online version of this article at:

<http://www.sciencemag.org/content/341/6152/1374.full.html>

Supporting Online Material can be found at:

<http://www.sciencemag.org/content/suppl/2013/09/18/341.6152.1374.DC1.html>

A list of selected additional articles on the Science Web sites **related to this article** can be found at:

<http://www.sciencemag.org/content/341/6152/1374.full.html#related>

This article **cites 33 articles**, 3 of which can be accessed free:

<http://www.sciencemag.org/content/341/6152/1374.full.html#ref-list-1>

This article has been **cited by** 1 articles hosted by HighWire Press; see:

<http://www.sciencemag.org/content/341/6152/1374.full.html#related-urls>

This article appears in the following **subject collections**:

Chemistry

<http://www.sciencemag.org/cgi/collection/chemistry>

References and Notes

- O. K. C. Tsui, T. P. Russell, C. J. Hawker, *Macromolecules* **34**, 5535–5539 (2001).
- C. J. Ellison, S. D. Kim, D. B. Hall, J. M. Torkelson, *Eur. Phys. J. E* **8**, 155–166 (2002).
- Y. Koh, G. McKenna, S. L. Simon, *J. Polym. Sci. B* **44**, 3518–3527 (2006).
- M. Efremov, E. Olson, M. Zhang, Z. Zhang, L. Allen, *Macromolecules* **37**, 4607–4616 (2004).
- E. U. Mapesa *et al.*, *Eur. Phys. J. Spec. Top.* **189**, 173–180 (2010).
- M. Tress *et al.*, *Macromolecules* **43**, 9937–9944 (2010).
- M. Erber *et al.*, *Macromolecules* **43**, 7729–7733 (2010).
- F. Kremer, E. U. Mapesa, M. Tress, M. Reiche, in *Recent Advances in Broadband Dielectric Spectroscopy*, Y. Kalmykov, Ed. (Springer, Dordrecht, Netherlands, 2013), pp. 163–178.
- R. B. Salazar, A. Shovskoy, H. Schönherr, G. J. Vancso, *Small* **2**, 1274–1282 (2006).
- M. Jaschke, H.-J. Butt, *Langmuir* **11**, 1061–1064 (1995).
- C. Acikgoz, M. A. Hempenius, G. Julius Vancso, J. Huskens, *Nanotechnology* **20**, 135304 (2009).
- J. Kumaki, Y. Nishikawa, T. Hashimoto, *J. Am. Chem. Soc.* **118**, 3321–3322 (1996).
- J. Kumaki, T. Hashimoto, *J. Am. Chem. Soc.* **125**, 4907–4917 (2003).
- A. Kiriý, G. Gorodyska, S. Minko, M. Stamm, C. Tsitsilianis, *Macromolecules* **36**, 8704–8711 (2003).
- M. E. McConney, S. Singamaneni, V. V. Tsukruk, *Pol. Rev.* **50**, 235–286 (2010).
- Y. Roiter, S. Minko, *J. Am. Chem. Soc.* **127**, 15688–15689 (2005).
- S. Capponi, S. Napolitano, M. Wübbenhorst, *Nat. Commun.* **3**, 1233 (2012).
- E. V. Russell, N. E. Israeloff, L. E. Walther, H. Alvarez Gomariz, *Phys. Rev. Lett.* **81**, 1461–1464 (1998).
- A. Sergei, F. Kremer, *Rev. Sci. Instrum.* **79**, 026101 (2008).
- F. Kremer, A. Schönhal, Eds., *Broadband Dielectric Spectroscopy* (Springer, Berlin, 2003).
- I. Bahar, B. Erman, F. Kremer, E. Fischer, *Macromolecules* **25**, 816–825 (1992).
- C. Iacob *et al.*, *Phys. Chem. Chem. Phys.* **12**, 13798–13803 (2010).
- S. Napolitano, M. Wübbenhorst, *Nat. Commun.* **2**, 260 (2011).
- G. Adam, J. Gibbs, *J. Chem. Phys.* **43**, 139 (1965).

Acknowledgments: We thank the Leibniz Institute of Polymer Research Dresden (IPF), especially P. Uhlmann and A. Lederer,

for conducting GPC measurements and A. Snytska for helpful discussions. Supported by the Graduate School BuildMoNa (M.T.), a Deutsche Forschungsgemeinschaft (DFG) grant within project SPP 1369 (E.U.M.), and DFG grant SFB TRR 102. A description of the sample preparation and the volume detection of the polymer coils, as well as details on the BDS and IR measurements, can be found in the supplementary materials. F.K. initiated and guided the project; M.R. was responsible for the fabrication of the nanostructured silicon wafers; M.T. and E.U.M. tested the suitability of the silicon wafers and developed the cleaning procedure; M.T. conducted the BDS experiments and AFM measurements, and analyzed the data; W.K.K. produced and filled the silica pores; W.K. performed and analyzed the IR measurements; and M.T., F.K., and E.U.M. wrote the manuscript.

Supplementary Material

www.sciencemag.org/content/341/6152/1371/suppl/DC1

Materials and Methods

Supplementary Text

Figs. S1 to S3

References (25–37)

9 April 2013; accepted 14 August 2013

10.1126/science.1238950

Lewis Acidity of Organofluorophosphonium Salts: Hydrodefluorination by a Saturated Acceptor

Christopher B. Caputo, Lindsay J. Hounjet, Roman Dobrovetsky, Douglas W. Stephan*

Prototypical Lewis acids, such as boranes, derive their reactivity from electronic unsaturation. Here, we report the Lewis acidity and catalytic application of electronically saturated phosphorus-centered electrophilic acceptors. Organofluorophosphonium salts of the formula $[(C_6F_5)_{3-x}Ph_xPF][B(C_6F_5)_4]$ ($x = 0$ or 1 ; Ph, phenyl) are shown to form adducts with neutral Lewis bases and to react rapidly with fluoroalkanes to produce difluorophosphoranes. In the presence of hydrosilane, the cation $[(C_6F_5)_3PF]^+$ is shown to catalyze the hydrodefluorination of fluoroalkanes, affording alkanes and fluorosilane. The mechanism demonstrates the impressive fluoride ion affinity of this highly electron-deficient phosphonium center.

Phosphorus(III) Lewis bases are widely exploited as ligands in transition metal coordination and organometallic chemistry; however, the electrophilic nature of phosphorus centers has garnered lesser attention. P(III) phosphonium cations have been explored by Gudat, Burford, and Ragogna, among others (1, 2). In recent computational work, phosphonium cations have been predicted to exhibit fluorophilicities comparable to those of known neutral Lewis acids, but substantially weaker than those of electrophilic cations such as $[Me_3Si]^+$ (Me, methyl) (3). Although P(V) Lewis acidity has been explored less (4), it is noteworthy that the P(V) centers in ylide reagents account for the classic Wittig reactions with ketones (5). Similarly, phosphonium cations have been used to facilitate additions to polar unsaturates (6) and Diels-Alder reactions (7). In related efforts, Hudnall *et al.* have also

recently exploited the acceptor capabilities of phosphonium cations, in tandem with boranes, to develop a series of fluoride ion sensors (8). Whereas these findings reveal the Lewis acidity of P cations, the chemistry of highly electrophilic phosphonium salts remains unexplored. Targeting such systems, we reported nucleophilic attack of a phosphine donor at an electron-deficient organofluorophosphonium salt (9, 10), leading to the phosphonium-difluorophosphorane product $[Ph_3P(1,4-C_6F_4)Ph_2PF_2][O_3SCF_3]$ (Ph, phenyl) (9). This behavior is reminiscent of the reactivity of $B(C_6F_5)_3$ (11), suggesting that $[(C_6F_5)_2Ph_2PF]^+$ and $B(C_6F_5)_3$ have similar Lewis acidity. Nonetheless, in contrast to the electrophilic nature of borane species, which is derived from the presence of a vacant p orbital, the Lewis acidity of organofluorophosphonium cations resides in the σ^* acceptor orbital oriented opposite the fluoride substituent (12). Further, the trigonal planar, electronically unsaturated nature of borane Lewis acids make them reactive toward most donor molecules. In contrast, phosphonium cat-

ions are electronically saturated and contain a P center that is sterically shielded by a pseudo-tetrahedral arrangement of substituents. As a consequence, most phosphonium salts are unreactive toward electron donors. Herein, the incorporation of electrophilic substituents at P is shown to afford highly Lewis acidic phosphonium centers. As a demonstration of their particularly strong fluorophilicity, these organofluorophosphonium cations are shown to directly activate C–F bonds and to effect the catalytic hydrodefluorination (HDF) of fluoroalkanes.

The electron-deficient phosphines $(C_6F_5)_2PhP$ and $(C_6F_5)_3P$ are cleanly oxidized with XeF_2 to give difluorophosphoranes $(C_6F_5)_2PhPF_2$ (1) and $(C_6F_5)_3PF_2$ (2) in quantitative yields. These species exhibit triplet resonances in their $^{31}P\{^1H\}$ nuclear magnetic resonance (NMR) spectra at chemical shifts $[\delta/\text{parts per million (ppm)}] -54.8$ and -48.0 , respectively, with a one-bond coupling constant ($^1J_{PF}$) of ~ 695 Hz. In contrast to the more electron-rich difluorophosphorane $(C_6F_5)_2Ph_2PF_2$ (13), neither 1 nor 2 undergoes fluoride ion abstraction by the Lewis acids $B(C_6F_5)_3$ or Me_3SiOTf (OTf, trifluoromethanesulfonate) (9, 10), leading to our inference that the targeted fluorophosphonium cations should exhibit comparatively stronger Lewis acidity. Nevertheless, 1 and 2 both undergo fluoride ion abstraction by $Al(C_6F_5)_3 \cdot C_7H_8$ (14) or $[Et_3Si][B(C_6F_5)_4] \cdot 2C_7H_8$ (Et, ethyl) (15, 16) to generate the corresponding fluorophosphonium salts $[(C_6F_5)_2PhPF]X$ [$X = [F(Al(C_6F_5)_3)_2]$, 3; $[B(C_6F_5)_4]$, 4] and $[(C_6F_5)_3PF]X$ [$X = [F(Al(C_6F_5)_3)_2]$, 5; $[B(C_6F_5)_4]$, 6], respectively (Fig. 1). Products 5 and 6 were easily identified by distinctive doublet resonances in their $^{31}P\{^1H\}$ NMR spectra at $\delta 77.7$ ($^1J_{PF} = 1042$ Hz) and 67.8 ($^1J_{PF} = 1062$ Hz) and in their ^{19}F NMR spectra at $\delta -121.9$ (doublet of pentets, $^1J_{PF} = 1042$ Hz) and -120.5 (doublet of septets, $^1J_{PF} = 1062$ Hz), respectively. The x-ray structure of 3 (Fig. 2A) clearly reveals the tetrahedral geometry of the

Department of Chemistry, University of Toronto, 80 St. George Street, Toronto, Ontario M5S 3H6, Canada.

*Corresponding author. E-mail: dstephan@chem.utoronto.ca

fluorophosphonium cation, with its P–F bond length of 1.533(2) Å. The anion contains an approximately linear Al(1)–F–Al(2) angle of 171.84(11)°, with Al(1)–F and Al(2)–F bond lengths of 1.788(2) and 1.780(2) Å, respectively. The cation and anion pack in the solid state such that the P–F(2) bond is oriented along the Al(1)–F–Al(2) vector with an F(2)⋯Al(1) interatomic separation of 3.677(2) Å, well within the sum of the van der Waals radii of these nuclei (3.98 Å). This interesting feature may be suggestive of π -stacking interactions between arenes of the cation and anion and/or of a weak dative F(2)→Al(1) attraction, consistent with the well-known hypervalency of Al.

Recognizing that **5** and **6** should incorporate the most electron-deficient P centers, efforts were made to gauge their Lewis acidity. Treatment of **6** with excess *N,N*-dimethylformamide (DMF) in CD₂Cl₂ solution gave rise to a new high-field doublet in the ³¹P{¹H} NMR spectrum at δ –46.7 with ¹*J*_{PF} = 705 Hz. The ¹⁹F NMR spectrum of this sample shows a downfield shift of the corresponding P–F signal to δ –3.6. These data demonstrate DMF coordination to the cation of **6**, affording the salt [(Me₂NC(O)H)(C₆F₅)₃PF][B(C₆F₅)₄] (**7**). Although **7** is generated in the presence of excess DMF, it was not isolable. Nonetheless, coordination of DMF demonstrates the Lewis acidity

(**7**) of the phosphonium cation and stands in contrast to simple alkyl- or aryl-phosphonium species. Efforts to employ more conventional Lewis acidity tests were also undertaken. Addition of crotonaldehyde to **6** as prescribed by Childs' method (**17**) resulted in a mixture of unidentified products. In contrast, following the Gutmann protocol (**18**), the combination of **6** and Et₃PO was monitored by ³¹P NMR spectroscopy. Adding 1 equivalent of Et₃PO to a CD₂Cl₂ solution of **6** at ambient temperature generated the adduct [(Et₃PO)(C₆F₅)₃PF][B(C₆F₅)₄] (**8**) (Fig. 1), as evidenced by two new doublet-of-doublet signals in the ³¹P{¹H} NMR spectrum at δ _p –51.3 (¹*J*_{PF} = 674 Hz, ²*J*_{PP} = 66 Hz) and 91.1 (²*J*_{PP} = 66 Hz, ³*J*_{PF} = 7 Hz). The latter resonance was attributed to the coordinated Et₃PO unit and is shifted downfield from that of free Et₃PO (δ _p 50.7). This shift (Δ = 40.4 ppm) is considerably larger than that observed when B(C₆F₅)₃ and Et₃PO are combined (Δ = 26.6 ppm), suggesting that the cation of **6** is ~1.5 times more Lewis acidic than B(C₆F₅)₃ on the Gutmann scale. To further probe the Lewis acidic nature of **5** and **6**, the geometry of the cation was optimized at the wb97XD/def2-TZVPP level of theory (see supplementary materials). The lowest unoccupied molecular orbital (LUMO) of **5** and **6** is concentrated on the P center (Fig. 2B). The major component occupies

space opposite the P–F bond and is sheltered by the arene rings. Smaller components of the LUMO reside at the ortho and para positions of these groups and at the P-bound F atom.

Another demonstration of the Lewis acidity of **6** is derived from its reaction with Ph₃CF. Combining **6** with Ph₃CF (**19**) in a 1:1 ratio in CD₂Cl₂ results in an instantaneous coloration of the reagents to produce a yellow-orange solution. The resulting ¹H NMR spectrum shows conversion of Ph₃CF to [Ph₃C][B(C₆F₅)₄], whereas ¹⁹F and ³¹P{¹H} NMR spectra demonstrate the formation of **2** (see supplementary materials). Reactions of **6** with fluoroalkanes are not limited to systems that generate stable carbocations. Indeed, **6** was also shown to react immediately with 1-fluoropentane, producing **2**, as confirmed by x-ray analysis of crystals isolated from the reaction mixture (**13**). The reactive *n*-pentyl cation generated by this process gave rise to unidentified side products arising from its reaction with [B(C₆F₅)₄][–], as has been observed previously (**20**). In a similar fashion, the addition of excess α,α,α -trifluorotoluene to solid **6** showed a more gradual conversion to **2**, along with slower degradation of the [B(C₆F₅)₄][–] anion, as noted above.

The aforementioned reactivity was subsequently exploited for HDF reactions using the phosphonium salt **6** as a catalyst. Fluoroalkanes were combined with Et₃SiH in the presence of 1 mole percent (mol %) of **6** (Table 1) at room temperature. In this fashion, 1-fluoroadmantane, 1-fluoropentane, fluorocyclohexane, and α,α,α -trifluorotoluene are catalytically converted to the corresponding hydrocarbons within 3 hours, whereas 1,4-*bis*(difluoromethyl)benzene required 24 hours, as evidenced by disappearance of the C–F resonances and appearance of the Et₃SiF signal in the ¹⁹F NMR spectra (see supplementary materials). In some cases, additional substituent redistribution affords small amounts of Et₂SiF₂ and Et₄Si, similar to that previously observed (**21**). Interestingly, octafluorotoluene could be converted exclusively to pentafluorotoluene (C₆F₅CH₃) and related products (**22**), demonstrating selective activation of the C(sp³)–F groups, and retention of C(sp²)–F groups. The substrates 1-bromo-3,5-*bis*(trifluoromethyl)benzene and 1,3,5-*tris*(trifluoromethyl)benzene also undergo

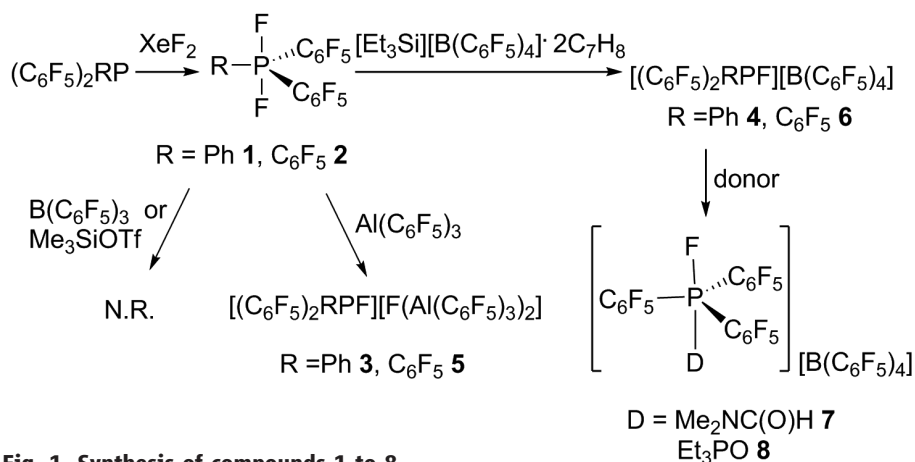
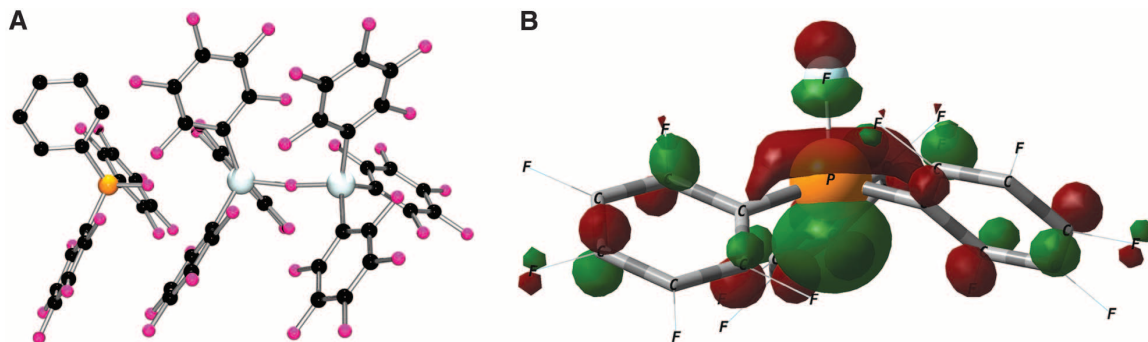


Fig. 1. Synthesis of compounds 1 to 8.

Fig. 2. Crystallography and electronic structure of fluorophosphonium salts. (A) Persistence of Vision Raytracer depiction of **3**. C, black; Al, blue-gray; F, pink; P, orange. All hydrogen atoms are omitted for clarity. (B) Graphical presentation of the LUMO of [(C₆F₅)₃PF]⁺ calculated at the wb97XD/def2-TZVPP level of theory (surface iso-value = 0.05).



HDF in this manner, although higher catalyst loadings (5 mol %) were required, an observation that is consistent with the greater number of C–F bonds present in these substrates. Nevertheless, using 10 mol % of **6** resulted in complete defluorination of these substrates after 24 hours. Previous reports have described C–F bond cleavage and catalytic HDF of fluoroalkanes by conventional, main-group Lewis acids such as $B(C_6F_5)_3$ (**23**), silylium (**20**), carbenium (**24**), and aluminum cations (**25**), though not by phosphonium salts.

We probed the mechanism of the HDF reaction. Combining $HSiEt_3$ and **6** resulted in no reaction, even on standing for several weeks as evidenced by $^{31}P\{^1H\}$ and ^{19}F NMR spectra. This observation is contrary to a mechanism involving hydride abstraction from silane by **6**, generating silylium cation, a known HDF catalyst (**26**). In sharp contrast, reactions of fluoroalkanes with the Lewis acidic phosphonium ion **6** lead to immediate C–F bond activation to produce intermediate difluorophosphorane **2** and a carbocation. In the catalytic process, the carbocation is quenched by the hydrosilane to afford an alkane and a transient silylium ion, which abstracts fluoride from phosphorane **2** to regenerate active catalyst **6** (Fig. 3). Further support for this proposition was obtained by a direct-competition experiment. Adding 1 equivalent of $[Et_3Si][B(C_6F_5)_4] \cdot 2C_7H_8$ to a 1:1 mixture of **2** and $C_6F_5CF_3$ in C_6H_5Br led to the immediate precipitation of **6** with no spectroscopic evidence for C–F bond activation after 10 min (see supplementary materials). This observation demonstrates that the fluoride ion in **2** is more labile than the alkyl C–F bond, supporting the proposition that catalyst **6** is regenerated by fluoride ion abstraction from **2**.

Additional support for this mechanism was acquired computationally at the $wB97XD/def2-TZVPP$ level of theory (gas phase) (**27**, **28**). We considered two conceivable reaction pathways and found hydride abstraction from Me_3SiH by $[(C_6F_5)_3PF]^+$ (+30.2 $\text{kcal}\cdot\text{mol}^{-1}$) to be much more endothermic than fluoride abstraction from $tBuF$ (+12.1 $\text{kcal}\cdot\text{mol}^{-1}$; *t*, tert). In either case, regeneration of catalyst **6** with production of alkane and fluorosilane is substantially exothermic, with a change in enthalpy ΔH value of $-44.9 \text{ kcal}\cdot\text{mol}^{-1}$. These computed energies support a reaction mechanism whereby the cation of **6** catalyzes HDF by directly activating the C–F bond of the fluoroalkane (see supplementary materials).

The ability of **6** to activate strong C–F bonds (bond energy = $\sim 490 \text{ kJ/mol}$) (**29**) and effect HDF catalysis results from the fluorophilicity of the organofluorophosphonium cation. Such reactivity is potentially important, as chlorofluorocarbons, hydrofluorocarbons, and perfluorocarbons (**30**) are persistent greenhouse gases. Indeed, transition metal reagents and catalysts have been developed to effect stoichiometric cleavage of C–F bonds and to bring about HDF catalysis (**31**, **32**). Metal-free strategies to HDF catalysis have also been pursued, exploiting highly Lewis acidic, electronically unsaturated species, including sili-

con cations (R_3Si^+), carbocations, aluminum ions (R_2Al^+), organoaluminum species, and $B(C_6F_5)_3$ (**33**). Though the silylium catalysts show greater activity (**20**), the present development of electron-

deficient organofluorophosphonium salts exploits electron-withdrawing substituents to generate enhanced Lewis acidity derived from a σ^* orbital of an electronically saturated species. The result-

Table 1. Catalytic hydrodefluorination of fluoroalkanes. R, alkyl; TON, turnover number.

$R-F + Et_3SiH \xrightarrow{6} R-H + Et_3SiF$					
Substrate	Cat. (mol %)*	t (h)	%Si–F [†]	%C–F [‡]	TON
Adamantyl–F	1	1	84	100	100
$C_5H_{11}F$	1	2	88	100	100
$C_6H_{11}F$	1	1	>95	100	100
$PhCF_3$	1	3	>95	>99	33
$1,4-C_6H_4(CF_2H)_2$	1	24	81	87	3.6
$C_6F_5CF_3$	1	24	71	98	4.1
$3,5-C_6H_3Br(CF_3)_2$	5	24	67	91	0.76
	10		77	>98	0.41
$1,3,5-C_6H_3(CF_3)_3$	5	24	49	69	0.58
	10		73	>99	0.41

*Relative to fluoroalkane substrate. †Calculated from the proportion of C–F bonds originally present relative to Si–F bonds formed. ‡Calculated from the proportion of C–F bonds consumed after time *t* (in hours). Conversions were determined by ^{19}F NMR spectroscopy using fluorobenzene as an internal standard.

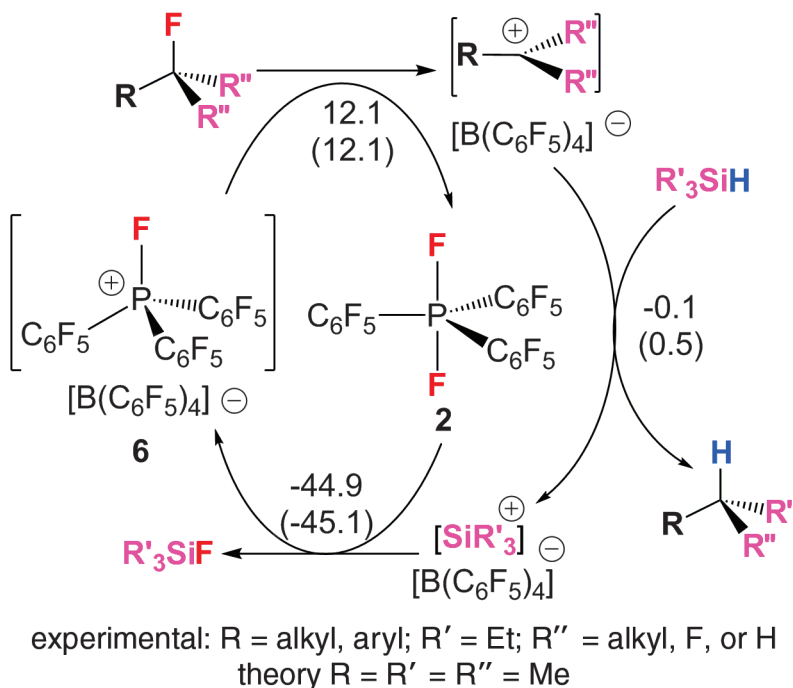


Fig. 3. Proposed reaction mechanism for phosphonium-catalyzed HDF reactions. Energies are calculated at the $wB97XD/def2-TZVPP$ level of theory. Energy values are given in units of kilocalories per mol relative to the energy of the $[(C_6F_5)_3PF]^+$, Me_3SiH , and $tBuF$ compounds; Gibbs free energies are given in parentheses.

ing electrophilic P cation coordinates donors and activates C(sp³)-F bonds of fluoroalkanes in both stoichiometric and catalytic reactions. The mechanism for this HDF catalysis illustrates the highly fluorophilic nature of these stable and readily accessible cations.

References and Notes

- D. Gudat, *Acc. Chem. Res.* **43**, 1307–1316 (2010).
- N. Burford, P. J. Ragona, *ACS Symp. Ser.* **917**, 280–292 (2005).
- J. M. Slattery, S. Hussein, *Dalton Trans.* **41**, 1808–1815 (2012).
- T. Werner, *Adv. Synth. Catal.* **351**, 1469–1481 (2009).
- G. Wittig, U. Schöllkopf, *Chem. Ber.* **87**, 1318–1330 (1954).
- O. Sereida, S. Tabassum, R. Wilhelm, *Top. Curr. Chem.* **291**, 349–393 (2010).
- M. Terada, M. Kouchi, *Tetrahedron* **62**, 401–409 (2006).
- T. W. Hudnall, Y. M. Kim, M. W. P. Bebbington, D. Bourissou, F. P. Gabbaï, *J. Am. Chem. Soc.* **130**, 10890–10891 (2008).
- L. J. Hounjet, C. B. Caputo, D. W. Stephan, *Dalton Trans.* **42**, 2629–2635 (2013).
- L. J. Hounjet, C. B. Caputo, D. W. Stephan, *Angew. Chem. Int. Ed.* **51**, 4714–4717 (2012).
- G. C. Welch, R. R. San Juan, J. D. Masuda, D. W. Stephan, *Science* **314**, 1124–1126 (2006).
- K. C. K. Swamy, N. S. Kumar, *Acc. Chem. Res.* **39**, 324–333 (2006).
- G. M. Sheldrick, *Acta Crystallogr. B* **31**, 1776–1778 (1975).
- G. S. Hair, A. H. Cowley, R. A. Jones, B. G. McBurnett, A. Voigt, *J. Am. Chem. Soc.* **121**, 4922–4923 (1999).
- J. B. Lambert, S. Zhang, S. M. Ciro, *Organometallics* **13**, 2430–2443 (1994).
- M. Nava, C. A. Reed, *Organometallics* **30**, 4798–4800 (2011).
- R. F. Childs, D. L. Mulholland, A. Nixon, *Can. J. Chem.* **60**, 801–808 (1982).
- V. Gutmann, *Coord. Chem. Rev.* **18**, 225–255 (1976).
- F. J. Weigert, *J. Org. Chem.* **45**, 3476–3483 (1980).
- C. Douvris, O. V. Ozerov, *Science* **321**, 1188–1190 (2008).
- V. J. Scott, R. Celenligil-Cetin, O. V. Ozerov, *J. Am. Chem. Soc.* **127**, 2852–2853 (2005).
- M. I. Bruce, *J. Chem. Soc. A* **1968**, 1459–1464 (1968).
- C. B. Caputo, D. W. Stephan, *Organometallics* **31**, 27–30 (2012).
- M. Alcarazo, C. Gomez, S. Holle, R. Goddard, *Angew. Chem. Int. Ed.* **49**, 5788–5791 (2010).
- W. Gu, M. R. Haneline, C. Douvris, O. V. Ozerov, *J. Am. Chem. Soc.* **131**, 11203–11212 (2009).
- C. Douvris, C. M. Nagaraja, C.-H. Chen, B. M. Foxman, O. V. Ozerov, *J. Am. Chem. Soc.* **132**, 4946–4953 (2010).
- J.-D. Chai, M. Head-Gordon, *Phys. Chem. Chem. Phys.* **10**, 6615–6620 (2008).
- S. Grimme, *J. Comput. Chem.* **27**, 1787–1799 (2006).
- M. F. Kuehnle, D. Lentz, T. Braun, *Angew. Chem. Int. Ed.* **52**, 3328–3348 (2013).
- K. P. Shine, W. T. Sturges, *Science* **315**, 1804–1805 (2007).
- A. Nova, R. Mas-Balleste, A. Lledos, *Organometallics* **31**, 1245–1256 (2012).
- T. Stahl, H. F. T. Klare, M. J. Oestreich, *J. Am. Chem. Soc.* **135**, 1248–1251 (2013).
- T. Stahl, H. Klare, M. Oestreich, *ACS Catal.* **2013**, 1578–1587 (2013).

Acknowledgments: D.W.S. gratefully acknowledges the financial support of the Natural Sciences and Engineering Research Council (NSERC) of Canada and the award of a Canada Research Chair. C.B.C. is grateful for the support of an NSERC-CGS-D Scholarship. Metrical parameters for the solid-state structure of compound **3** are available free of charge from the Cambridge Crystallographic Data Centre under reference number CCDC-951501.

Supplementary Materials

www.sciencemag.org/content/341/6152/1374/suppl/DC1
Materials and Methods
Supplementary Text
Figs. S1 to S16
References

11 June 2013; accepted 9 August 2013
10.1126/science.1241764

Deep-Focus Earthquake Analogs Recorded at High Pressure and Temperature in the Laboratory

Alexandre Schubnel,^{1*} Fabrice Brunet,² Nadège Hilairiet,^{3†} Julien Gasc,³ Yanbin Wang,³ Harry W. Green II⁴

Phase transformations of metastable olivine might trigger deep-focus earthquakes (400 to 700 kilometers) in cold subducting lithosphere. To explore the feasibility of this mechanism, we performed laboratory deformation experiments on germanium olivine (Mg₂GeO₄) under differential stress at high pressure ($P = 2$ to 5 gigapascals) and within a narrow temperature range ($T = 1000$ to 1250 kelvin). We found that fractures nucleate at the onset of the olivine-to-spinel transition. These fractures propagate dynamically (at a nonnegligible fraction of the shear wave velocity) so that intense acoustic emissions are generated. Similar to deep-focus earthquakes, these acoustic emissions arise from pure shear sources and obey the Gutenberg-Richter law without following Omori's law. Microstructural observations prove that dynamic weakening likely involves superplasticity of the nanocrystalline spinel reaction product at seismic strain rates.

The origin of deep-focus earthquakes fundamentally differs from that of shallow (<100 km) earthquakes (*1*), for which theories of rock fracture rely on the properties of coalescing cracks and friction (*2–4*). As pressure and temperature increase with depth, intracrystalline plasticity dominates the deformation

regime so that rocks yield by creep or flow rather than by brittle fracturing (*4*). Polymorphic phase transitions in olivine have provided an attractive alternative mechanism for deep-focus earthquakes (*5, 6*). For instance, transformation of olivine to its high-pressure polymorphs could induce faulting in polycrystalline Mg₂GeO₄ olivine (*7, 8*). This was further confirmed on silicate olivine, (Mg,Fe)₂SiO₄, during the olivine-wadsleyite transition (*9*). Additional experiments demonstrated that the mechanism produced acoustic emissions (AEs) (*10*).

In total, we performed eight experiments on both powdered and sintered Ge-olivine samples in the stability field of the spinel polymorph, at confining pressures from 2 to 5 GPa and temperatures between 973 and 1573 K (fig. S2). Sintered

samples consisted of fully densified “rocks” of isostatically hot pressed polycrystalline Mg₂GeO₄ (Ge-olivine) containing minor amounts of Gepyroxene (<5 vol %) (*11*). We used the germanate analog of Mg₂SiO₄ olivine because transformation into its denser polymorph can be reached at pressures routinely achievable in the deformation apparatus. Stress, transformation progress, and strain were measured in situ by using x-ray powder diffraction (XRD) and radiographic imaging, respectively. AEs were recorded continuously on six channels. Description of the set-up is given in the supplementary materials (fig. S1) (*12*).

Differential stress, strain, and acoustic activity for sample D1247 evolved as a function of time (Fig. 1). The sample was first pressurized to 4 GPa at room temperature then deformed at a constant temperature of 973 K with a strain rate

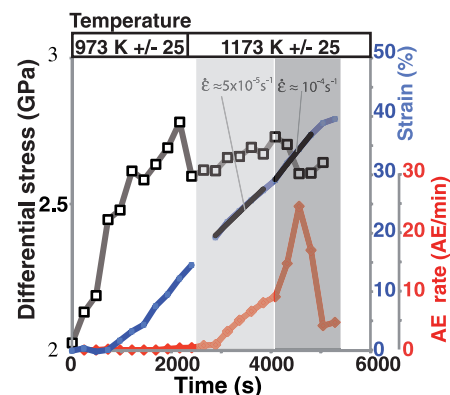


Fig. 1. Stress, strain and acoustic emission. Evolution of temperature, differential stress, strain, and AE rate during experiment D1247 performed at 4 GPa effective mean stress.

¹Laboratoire de Géologie, CNRS UMR 8538, Ecole Normale Supérieure, 75005 Paris, France. ²Institut des Sciences de la Terre, CNRS, Université de Grenoble 1, 73370 Grenoble, France. ³GeoSoilEnviroCARS, University of Chicago, Argonne, IL 60439, USA. ⁴Department of Earth Sciences, University of California at Riverside, CA 92507, USA.

*Corresponding author. E-mail: aschubnel@geologie.ens.fr
†Present address: Unité Matériaux et Transformations, CNRS UMR 8207, Université Lille 1, 59655 Villeneuve d'Ascq, France.